

DYNAMICS LAGOON MODELING USING DETAILED TIME-SERIES DIGITAL TERRAIN MODEL

Atriyon Julzarika^{1*} , Nanin Anggraini¹, Argo Galih Suhadha^{1,2}, Danang Budi Susetyo^{1,3},
Rahmadi Rahmadi¹, Bayu Prayudha¹, Nugroho Purwono¹, Yaya Ihya Ulumuddin¹

¹*The National Research and Innovation Agency (BRIN), Cibinong, Indonesia*

²*Tohoku University, Sendai, Japan*

³*Yildiz Technical University, Istanbul, Türkiye*

*verbhakov@yahoo.com

Abstract: A lagoon is a natural feature formed at the mouth of a river due to the dynamics of river sedimentation, currents, vertical deformation, waves, and tides. Lagoons are dominated by soft soil, so their topography is dynamic. Segara Anakan Lagoon (SAL) is an area that experiences dynamic topography caused by rapid sedimentation. Changes in the dynamics of the delta topography can be tracked in the past with the Digital Terrain Model (DTM) time series extracted from the latest DTM, vertical deformation, and sedimentation data. The observation period was 1978–2021. This study aims to model topography dynamics (1978–2021) in SAL according to DTM, vertical deformation, and sedimentation data. This dynamics topography modeling uses (1) parameters of sedimentation rate and volume obtained from river basin center – *Balai Besar Wilayah Sungai* (BBWS) 2012, (2) DTM 2021 extracted from ALOS-2 (2017) and integrated with vertical deformation from Sentinel-1 (2017–2021) using the Differential Interferometry Synthetic Aperture Radar (D-InSAR) method. The DTMs (1978, 1991, 2001, and 2010) are extracted using a geospatial forensics approach based on topography modeling of DTM 2021, vertical deformation (2017–2021), and rapid sedimentation data. We use the sediment rate entering SAL from the Citanduy River (8.05 million tons/year), Cimeneng River (0.87 million tons/year), and Cikonde River (0.22 million tons/year), with a total sediment supply of 9.14 million tons/year. The DTM 2021 has a spatial resolution of 1 m and has been validated in its vertical accuracy test (+17.6 cm) and its height difference test (~0 m) with a confidence level of 95 % (1.96 σ). The average vertical deformation value is –0.0240 to –0.0320 m. The results obtained are dynamics topography information (1978–2021). The DTMs (1978–2021) visualize dynamics topography changes in SAL. They are carried out by checking the dynamics of shoreline changes and cross-section profiles to determine the suitability of shapes and patterns (lagoon and delta). Sedimentation is the most significant parameter that influences the topography dynamics in SAL.

Key words: DTM and vertical deformation; dynamic lagoon; SAL; dynamics topography; rapid sedimentation

1. INTRODUCTION

A lagoon is a body of relatively shallow salt water separated from larger bodies of water by sandbars, barrier reefs, coral reefs, barrier islands, barrier peninsula, isthmus, or other natural barriers (NOAA, 2024). Lagoons form around river mouths that carry large amounts of sediment (Ardli, 2008). Lagoons can be categorized as coastal lagoons and atoll lagoons (Spaulding, 1994). Coastal lagoons (barrier lagoons) are formed by sand or coral on shallow beaches, while atoll lagoons are formed by coral reef growth. A typical lagoon is characterized by having water enclosed behind coral reefs or islands or within an atoll.

Coastal lagoons are generally shallow waters influenced by the sea. Ecologically and economically, coastal lagoons are important due to their high

productivity and intensive human use for waste disposal, recreation, and aquaculture (Spaulding, 1994). Islands formed in front of these river mouths form deltaic deposits. The location of the deltaic deposits is partly within the delta (flood tidal delta) and partly in the open sea (ebb-tidal delta) (Şenol et al., 2024).

Multi-source geospatial data technology can be used to map and monitor the lagoon's dynamics (Karim et al., 2019; Şenol et al., 2024). A dynamic lagoon is a topographic condition in the lagoon over a time series. Studies related to lagoon dynamics help understand the topographic track record in the study area, including the formation process, topographic dynamics, land changes, and the influence of the dynamics of the Earth's processes.

The problems so far in topographic mapping in the lagoon area are the need for wide area coverage, remote area, lack of data availability, outdated data, not detailed, high costs, and long, time-consuming mapping (Paul et al., 2014). The large lagoon requires wide coverage of geospatial technology, such as satellite imagery or aerial photography, integrated with field measurement data (Şenol et al., 2024). High precision is obtained from mapping with wide coverage geospatial technology (satellite and aerial). In contrast, high accuracy is obtained from mapping with large-scale geospatial technology, such as geodetic measurements in the field (Arroyo-Ortega et al., 2024).

The research location is the Segara Anakan Lagoon (SAL), Cilacap Regency, Province of Central Java, Indonesia. SAL is an example of a large dynamic lagoon and delta located along the southern coast of Java Island (Prayudha et al., 2021). It is located at 108.7715860, -7.6158540 to 109.0966440, -7.8073350 (see Figure 1). The location selection was based on the very high dynamics of Lagoon change due to sedimentation. The lagoon is linked to the Hindian Ocean through a western outlet known as Plawangan, and it also has an eastern outlet leading towards Cilacap via a tidal channel.

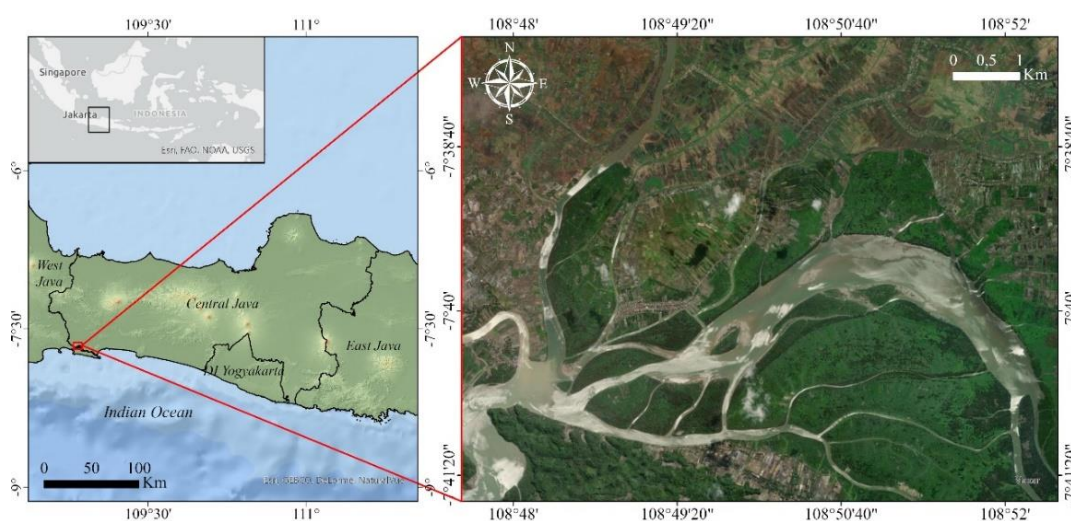


Fig. 1. Segara Anakan Lagoon, Indonesia. Satellite imagery from Google Earth

The central and western regions of the lagoon have very shallow depths, often less than 2 meters. However, in the far western part, stretching from the mouth of the Citanduy River to the Hindian Ocean, deeper waters can be found, with the Plawangan channel reaching over 10 meters in depth. In the eastern part of the lagoon, the Sapuregel and Donan branches have water depths ranging from 5 to 10 meters, mainly due to limited freshwater and sediment inflow. The western lagoon area receives significant amounts of freshwater, including suspended sediments, from various sources like the Citanduy River, Cikujang River, Cikonde River, and Cibeureum River. The Citanduy River is especially important as the main river in the Citanduy watershed, which is vital for hydrology and erosion processes. Unfortunately, the lagoon is experiencing rapid sediment buildup caused by high soil erosion rates in upland areas. These environmental changes and the reduction in lagoon space have negatively

impacted fishery yields, compared to the effects on fishery yields (Dudley, 2000).

Lagoons hold high ecological and economic value because of the richness and diversity of their natural biological resources (Ismail, et al. 2018). They include commercially important fish, crabs, and mangroves. Over the past few decades, coastal habitats in this region have changed due to increased urbanization and the expansion of agricultural and aquaculture activities, leading to issues such as rural encroachment on farmland, reclamation of swamps, silt deposition in lagoons, and a decline in capture fisheries (Akbar et al., 2020; Prayudha et al., 2021). The surrounding environmental conditions along the watershed influence the estuary waters, resulting in significant pollution and sedimentation (Dsikowitzky et al., 2018; Prayudha et al., 2021).

One of the exciting aspects of SAL is the silting process due to sedimentation that occurs in the lagoon (Akbar et al., 2020). Large rivers such as

Citanduy, Cikonde, Cimeneng, Cibeureum, Sapuregel, Donan, and several other rivers the influence of land is very dominant in the deposition process, and several tributaries that flow into the area (Prayudha et al., 2021). These rivers carry sedimentary material resulting from upstream erosion and are deposited at the river mouth. 65% of the sediment that settles in SAL comes from the Citanduy River, and the rest flows into the sea via West Pelawangan (Ongkosongo, 1986; Prayudha et al., 2021). The SAL is a narrow outlet and bends, so much material carried towards the high seas is deposited on the inside of the river bend. Coupled with the wave energy from the high seas, which is stronger than the energy the river carries, sediment is deposited back towards the mainland. There have been many studies related to sedimentation that occurred in the SAL and its delta.

Changes in the shape of SAL can be monitored by paying attention to the orthometric height (elevation) of the land. Topography is one factor that controls the processes that occur in layers on the Earth's surface (Julzarika & Djurdjani, 2018; Strozzi, T., Klimeš, J. et al., 2018; Wilson, 2012). The altitude of the land can be estimated using Digital Terrain Models (DTMs). DTM is a digital elevation model without vegetation and building surfaces and has been equipped with rivers, contours, and natural features (ASPRS, 2014; Li et al., 2004; Maune & Nayegandhi, 2018). A DTM denotes the bare ground surface without any objects. Another definition of the it, DTM is a digital representation of the Earth's bare ground surface, providing elevation data for every point on the terrain by excluding features like buildings, trees, and other man-made objects, essentially creating a 3D model of the land topography used in fields like surveying, engineer-

ing, and environmental management (Guth et al., 2021). The DTMs are useful to perform several morphometric analysis such as for monitoring sedimentation in SAL. DTM can be obtained starting from several data. Examples of data sources used to extract DTM data are satellite image data, aerial photos, and Light Detection and Ranging (LiDAR) data (Julzarika & Djurdjani, 2018).

Previous studies on SAL have extensively documented its rapid shrinkage using 2D shoreline analysis from historical maps and satellite imagery, and have quantified sediment inflow from major rivers. However, these approaches often lack a crucial third dimension: vertical topographic change. Understanding the volumetric evolution and geomorphological dynamics requires detailed DTM time series. Such historical DTMs are typically unavailable, creating a significant data gap in modeling past landscape conditions. This study addresses this gap by introducing a geospatial forensic approach to reconstruct historical DTMs, thereby enabling a novel, quantitative 4D (3D space and time) analysis of the lagoon's dynamic topography, moving beyond simple area-based assessments.

In this work, we use satellite images to extract DTMs and vertical deformation and then model the geospatial forensics approach with rapid sedimentation data to extract the past DTMs (1978, 1991, 2001, 2010). The novelty of this research is modeling the dynamics of topographic change (1978–2021) in SAL based on DTM, vertical deformation, and rapid sedimentation data. This dynamic topography modeling uses (1) parameters of sedimentation rate and volume obtained from BBWS 2012, (2) DTM 2021 extracted from ALOS-2 (2017) and integrated with vertical deformation from Sentinel-1 (2017–2021) using the D-InSAR method.

2. METHODOLOGY

The data used in this study are ALOS-2 (2017), Sentinel-1 (2017–2021), and sedimentation rate data from river basin center – *Balai Besar Wilayah Sungai* – BBWS (2012). These data extract past DTMs (1978, 1991, 2001, and 2010). DTM (2021) is an integration DTM between DTM master (2017) and vertical deformation (2017–2021). The selection of processing years (1978, 1991, 2001, and 2010) is based on the conditions of extreme changes in the area's topography and information from several parties that the SAL underwent significant changes in shape during that period. We use the sedimentation rate data from BBWS Citanduy as

one of the parameter inputs to model the past DTMs. The rate of sediment entering SAL from the Citanduy River is 8.05 million tons/year, the Cimeneng River is 0.87 million tons/year, and the Cikonde River is 0.22 million tons/year, with a total sediment supply of 9.14 million tons/year (BBWS, 2012).

2.1. DTM and vertical deformation

The past DTMs were extracted using the dynamics DTM or the latest DTM method. This dynamics DTM method enables the DTM modeling

of past conditions and the prediction of future topography based on time-series data. The dynamics DTM combines the DTM master, extracted from the ALOS-2 images and WorldView-2 (2017), with vertical deformation data obtained from the Sentinel-1 image (2017–2021). The spatial resolution of ALOS-2 is 3 m, WorldView-2 (60 cm), and Sentinel-1 (10 m). The DTM master was derived using the Interferometry Synthetic Aperture Radar (InSAR) technique, while the vertical deformation was obtained through the Differential InSAR (D-InSAR) method (Dias et al., 2018; Julzarika et al., 2022; Julzarika & Harintaka, 2019; Nico et al., 2005; Strozzi, T., Klimeš, J., et al. 2018). The default DTM is 2021. DTM 2021, vertical deformation, and rapid sedimentation data are used to model the past DTMs. The selected years for past DTMs are 2010, 2001, 1991, and 1978.

Geospatial forensics (geoforensics) was carried out using geomodeling and geo-visualization approaches with basic data of DTM (topography and bathymetry) and deformation (vertical and horizontal) (Mazhari, 2010; Ruffell & McKinley, 2008). Sentinel-1 images were used for vertical deformation extraction. They are used for vertical deformation extraction with the D-InSAR method (Guzzeti et al., 2009; Liosis et al., 2018; Luca et al., 2018). The average vertical deformation value used in this modeling is 8–10 cm/year, based on D-InSAR Sentinel-1 and field measurements on Cilacap. We use the Global Navigation Satellite System (GNSS) to measure and compare their results with the vertical deformation data from Sentinel-1.

We use equation (1) to model the past topography (1978, 1991, 2001, 2010). Equation (2) is used to extract the dynamics of DTM 2021. The topography and bathymetry (DTM 2021) data have a spatial resolution of 1 m ($X = 1$ m; $Y = 1$ m; $Z = 1$ m). The DTM used must have vertical accuracy < 1 m with a confidence level of 1.96σ (95%) (ASPRS, 2014; Julzarika et al., 2021). The fixed shoreline between topography and bathymetry can be obtained after merging the data with the Digital Elevation (DEM) integration method (Hoja & D'Angelo, 2010; Julzarika et al., 2021; Li et al., 2017).

$$\text{Modeling of Past DTM} = \text{DTM}_{(2021)} - [\sigma_0^2 * \alpha] - [n * \beta] - [n * \gamma] - [\delta] + e \quad (1)$$

$$\text{DTM}_{(2021)} = \text{DTM master}_{(2017)} + \text{vertical deformation}_{(2017-2021)} \quad (2)$$

where:

$\text{DTM}_{(2021)} = \text{DTM}_{\text{integration}}$ (topography and bathymetry in 2021), $\text{DTM master}_{(2017)}$ extracted using InSAR of ALOS-2 (2017) and integrated with WorldView-2 (2017), vertical deformation extracted using D-InSAR Sentinel-1 (2017–2021),

$\sigma_0^2 =$ a posteriori variance,

$\alpha = (\text{DTM}_{(2021)} + \text{vertical deformation}_{(2017-2021)} - \text{horizontal deformation})$,

$\beta = (\sigma_{\text{dtm}2021} \sigma_{\text{vertical deformation}}) * \text{mean of vertical deformation}_{(2017-2021)}$,

$\gamma = (\sigma_{\text{dtm}2021} \sigma_{\text{horizontal deformation}}) * \text{mean of horizontal deformation}$,

$\delta = (\sigma_{\text{sedimentation}})^2 * \text{the rate of sedimentation volume}$,

In this research, we use a 95 % confidence level (1.96σ)

$n =$ the difference years between the past or future with 2021.

For example, if we want to model the past DTM in 1000 AD, the $n = 1021$.

$(\sigma_{\text{dtm}2021} \sigma_{\text{vertical deformation}}) =$ variant covariance between the latest DTM standard deviation with vertical deformation standard deviation,

$(\sigma_{\text{dtm}2021} \sigma_{\text{horizontal deformation}}) =$ variant covariance between the latest DTM standard deviation with horizontal deformation standard deviation,

$e =$ random errors.

All the parameter calculations are based on the least square adjustment computation.

The logic behind the past DTM modeling (Equation 1) is a retrodictive approach based on a mass balance principle. It assumes that the present-day topography (DTM 2021) is the cumulative result of past topography plus subsequent material deposition (sedimentation) and minus vertical displacement (subsidence). Therefore, we can mathematically reconstruct the historical terrain surface by systematically subtracting the estimated cumulative effects of sedimentation and vertical deformation over a specific period (n years) from the current DTM. Using least-squares adjustment and variance-covariance matrices is critical for integrating these multi-source datasets, weighting each parameter based on statistical uncertainty, and ensuring a robust model output.

Analysis of the landform and area changes of the SAL was carried out using the DTM. Land elevation data formed in the SAL indicates the addition

of land at that location. The DTM elevation information follows the orthometric height (elevation) with the Earth Gravitational Model (EGM) 2008 for its height reference field. Analysis of changes in shape and area of the SAL is obtained from the shoreline based on sea-level data with the Mean Sea Level (MSL) reference plane. A geoid plane is an equipotential plane that coincides with the MSL. This shoreline is based on measurements of the elevation 0 m at dynamics DTMs. The dynamics DTM results were validated by comparing the orthometric height data with GNSS-leveling data. Orthometric heights are compared with DTM 2021 to get the vertical accuracy assessment.

2.2. DEM integration and vertical deformation assessment

DEM integration is a method of integrating height data and/or n -dimensional data with weighting on each data based on the variance-covariance calculated by least square adjustment computation, see equation (3) (Hoja & D'Angelo, 2010; Julzarika et al., 2021). DEM integration combines data (DEM) by involving two or more datasets. The combination considers cofactor values and the variance-covariance between data (Hoja & D'Angelo, 2010; Julzarika et al., 2021). The calculation uses the adjustment method, where the number of measurements exceeds the number of parameters. (Ghilani & Wolf, 2006; Li et al., 2004).

$$\text{DEM Integration} = ((\sum hi * pi) / \sum pi) + \text{void filling the gaps} + \text{delta surface fill} + e \quad (3)$$

where: hi = elevation in number pixel;
 pi = weighted mean height in number pixel

The DTM and vertical deformation need to be tested for vertical accuracy assessment. It includes

a height difference test and a vertical accuracy test. The method is to check at least 25 height points on an area of 500 km² with a 95% confidence level (1.96σ) using GNSS-leveling. The vertical accuracy test refers to the ASPRS 2014 standard; see equation (4) (ASPRS, 2014). The vertical accuracy test aims to determine the maximum vertical value in a DTM that can be used on a map scale determined by specific mapping standards, such as ASPRS 2014. A cross-section profile check is conducted to see if the DTM meets the specified standards. The height difference test was carried out at 25 points made of polygons, and the sum of the height difference values between the polygon points was calculated. The height difference test aims to determine the vertical accuracy value at a certain tolerance so that it can be used to eliminate systematic errors that still exist in the height model (Hoja & D'Angelo, 2010). The height difference test can be useful in determining the height difference between two or more points, see equation (5).

$$\text{Vertical accuracy test} = 1.96 * [(\sum (H_{\text{data}} - H_{\text{check}})^2 / n)^{1/2}] \quad (4)$$

where: H = orthometric height; n = sum of height point (minimum 25 measurement points).

$$\text{Height different test} = \sum (H_{n1} - H_{n0}) \quad (5)$$

where: H_{n1} = the next height point in the polygon;
 H_{n0} = the before height point in the polygon.

The DTM 2021 is validated by comparison with GNSS-leveling measurements. The vertical accuracy test uses 25 measurement points because the area is still less than 500 km². The accuracy test includes a height difference test and a vertical accuracy test. The height difference test of DTM 2021 is ~ 0 m. The Root Mean Square Error Vertical (RMSE_z) is 0.17599097 m. The vertical accuracy test of DTM₍₂₀₂₁₎ is ± 17.6 cm ($1.96 * \text{RMSE}_z$) with a confidence level of 95 % (1.96σ).

3. RESULTS

The results of this study include the DTM master and vertical deformation. The DTM master was extracted from the ALOS-2 (2017). Vertical deformation is a visualization of vertical deformation from 2017 to 2021. DTM 2021 is an integration of DTM Master 2017 with vertical deformation (2017–2021). DTM 2021 is the latest DTM for 2021, and it is used as the main reference for topography (see Figure 2(A)). The vertical deformation (2017–2021) based on the tectonic movement in the

SAL area is between -0.0210 and -0.0340 m. Tectonically, the entire region is experiencing subsidence overall. The average subsidence value is in the range of -0.0240 to -0.0320 m.

Figure 2(A) is a dynamic topography change of the shoreline based on the time-series DTMs (1978–2021), and the sedimentation area forms land with a higher elevation of 0.5–1.8 m. The black line is the shoreline for 2021 based on an elevation of 0 m in DTM 2021. During this period, a shoreline or

elevation of 0 m is only found in rivers and estuaries in parts with cyan and blue colors (elevation < 0 m). The area still has less water compared to the topography of 2010, 2001, 1991, and 1978. The white line is the shoreline in the topography of 1978. The blue line is the shoreline in the topography of 1991, the red line is the shoreline in the topography of 2001, and the yellow line is the shoreline in the topography of 2010. During this period, the water area was still wide and covered almost the entire

SAL. It can be seen in Figure 2(A) that 1978 had only a little sedimentation compared to other years. In 1991, the land surface became wider and increased in height. It can be seen from the chart pattern of increasing elevation. We can see the rapid sediment change from 1978 to 2001. The most significant change in land height was in 2010 compared to the elevation in 1978. It can be seen from the yellow line that it is the highest compared to other lines.

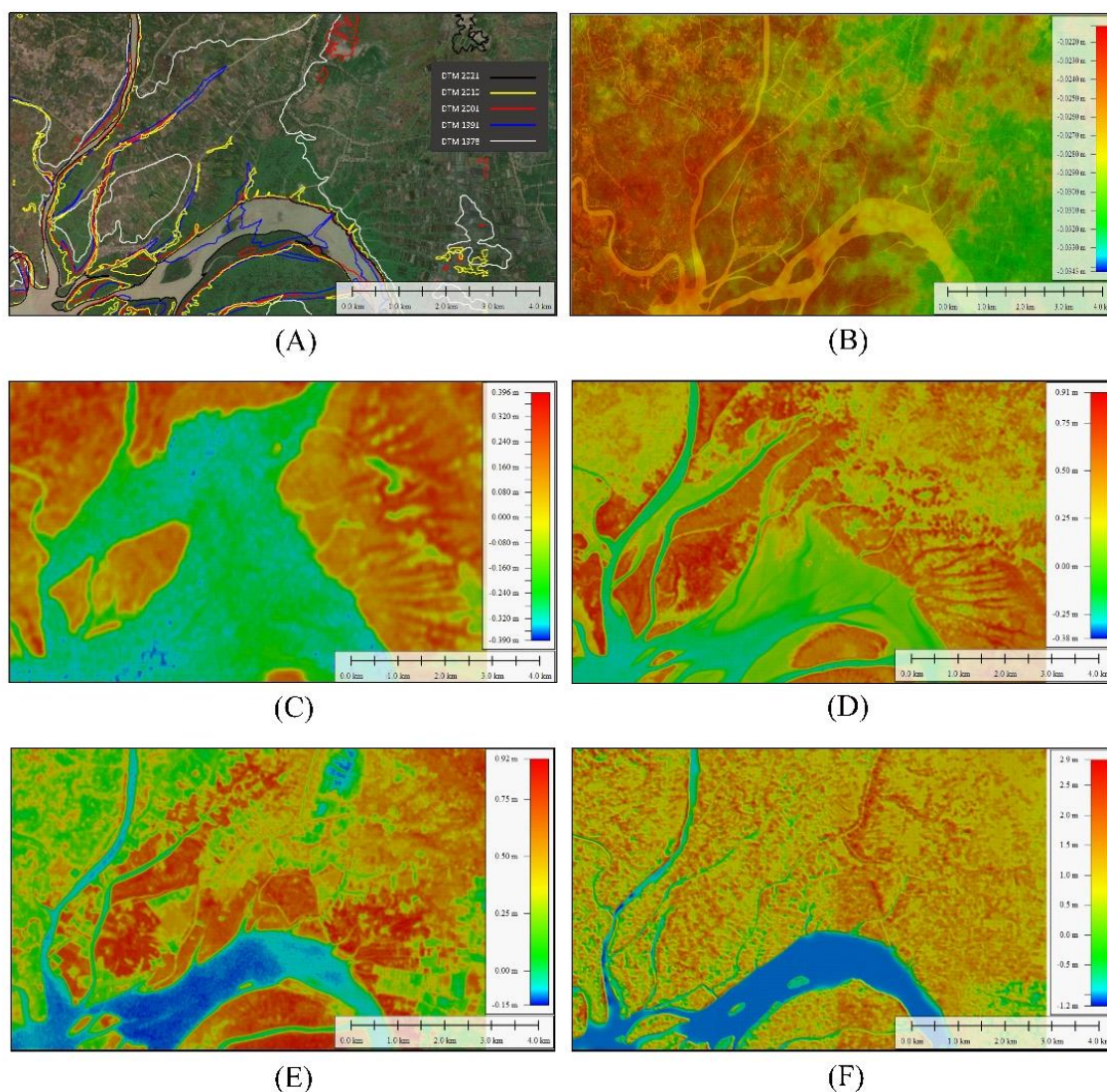


Fig. 2. Time-series DTM (1978, 1991, 2001, 2010, and 2021) with the cross-sections. (A): Super-dynamics shoreline change based on time-series DTM (1978–2021). Background topography using DTM 2021; (B): Vertical deformation 2017–2021; (C): DTM 1978; (D): DTM 1991; (E): DTM 2001; (F): DTM 2010

D-InSAR of Sentinel-1 extracts the vertical deformation (2017–2021) in the SAL area. It has a value between -0.0210 and -0.0340 m. Overall, the entire region is experiencing subsidence. The average subsidence value is in the range of -0.0240

to -0.0320 m. Figure 2(B) is the vertical deformation of SAL (2017–2021). Figure 2(C) is a view of the DTM 1978. In 1978, the SAL looked wider, and the river mouth in the area was more significant than in 2021. Large rivers and several tributaries carry

sediment particles, causing sedimentation to form soil. Based on the DTM analysis, the land elevation in the area is between 0.04 m and 0.36 m. The land on the lagoon's edge and the resulting raised land have a height of about 0.2 m. The length of the raised soil in SAL is 3 km, with a width of 1.5 km.

Figure 2(D) is the DTM 1991. In 1991, changes began to appear in SAL. The rising land in the DTM 1978 merged with the mainland on the north side to form a lagoon. The mouth of the river that looked wide in 1978 has narrowed and has turned into a new land. This significant change can be seen from the extent of the newly formed land and the area's topography. The length of the raised soil formed is 5.8 km, and the width is 2.4 km. The topography around the Lagoon appears to have increased, even though the height of the raised land since 1978 has increased to 0.97 m. The potential for the emergence of new emerging soils is getting bigger. This can be seen by the sedimentation deposits starting to be seen clearly on the east side and reaching a height of 0.8 m.

Figure 2(E) is the DTM 2001. The emerging land that has occurred is getting more comprehensive with a tendency towards the east, and there is a potential for emerging land to appear in the south. The width of the land rising in 2001 since 1978 has reached 2.9 km with a length of 7.8 km. The topography of the rising soil varies between 0.1 and 0.9

m, and the topography that leads to the mainland tends to increase. Figure 2(F) is the DTM 2010. In 2010, there was an increase in the length and thickness of the emergent soil, which had been joined to the mainland, although the width had not changed significantly. The length of the raised soil reaches 8.1 km and a width of 2.8 km. The raised ground height is very significant, reaching more than 2 m. The results of the DTM 2021 show the current condition of SAL (2021). The mouth of the river that looked wide in 1978 disappeared and became a new land. The length of the land formed until 2021 reaches 8.3 km with a width of 2.9 km. The height of the raised soil reaches 1.8 m.

Based on the cross-section profile, it can be seen that there is a high sedimentation rate in the river channel. The depth of the waters of the SAL in 1978 reached 0.3 m, and the depth of the river upstream is getting shallower. The waters of the SAL, which were initially very wide, became narrower due to sedimentation. Soil forms and begins to merge with the mainland, causing a channel to form that resembles a river. The formed river carries sediment particles, so the land arising in the SAL gets wider. Figure 3 is the cross-section profile of the time-series DTMs. The cross-section profile shows the dynamics of topography changing in the lagoon and new land in SAL.

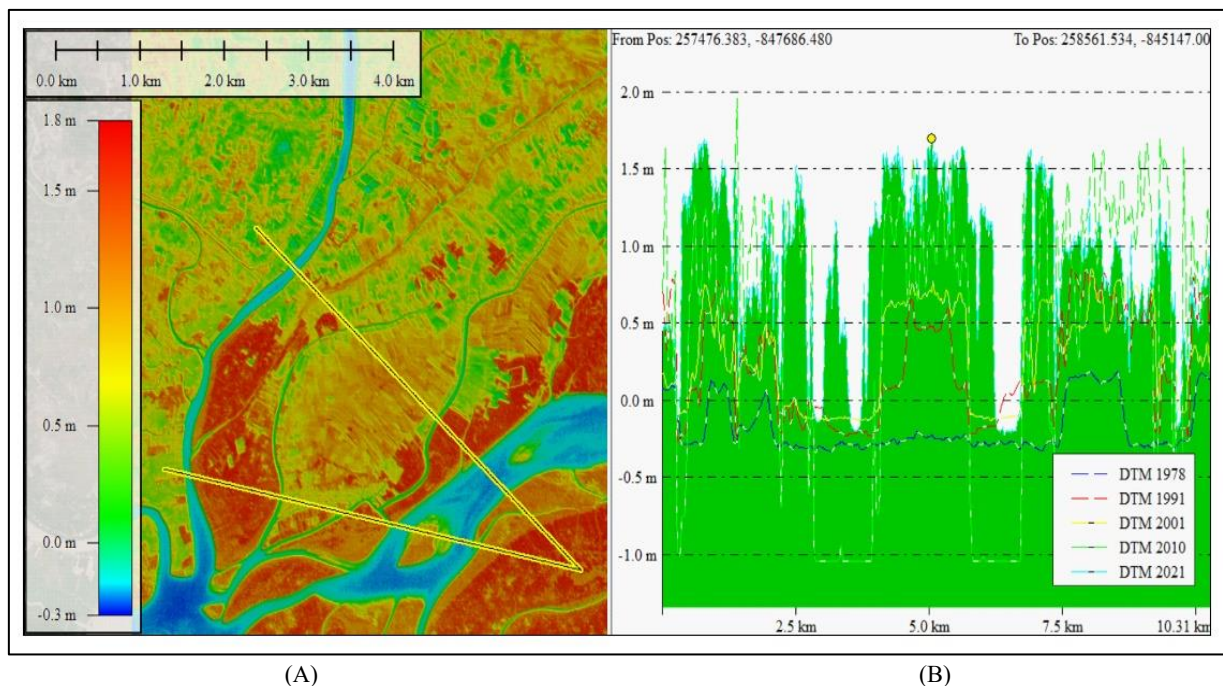


Fig. 3. (A): DTM (2021); the yellow line shows the cross-section.
(B): The terrain profile of the time series (1978–2021) is based on the cross-section (A).

An accuracy test was carried out using a cross-section profile test to determine the dynamic changes of topography sedimentation in SAL. Based on the results of the cross-section test, it is seen that there is a significant change in the land of SAL. The depth of the river channel in 1991 began to increase compared to 1978, but in some locations, the depth decreased. A significant increase in the river channel depth occurred in 2001 when the depth reached 0.04 m. It is presumably due to the high

sedimentation rate caused by damage from the upstream watershed. The river channel depth decreased again in 2010 and increased again in 2021. The depth of the river channel in 2010 reached -1.6 m. The decrease in depth is due to tectonic dynamics and soft soil in the study area. The sedimentation value remains higher than that of vertical deformation because the erosion rate from upstream is also high. The depth of the river channel in 2021 will reach 0.6 m.

4. DISCUSSION

Many factors caused topographic changes in that period due to rapid high sedimentation, changes in river and sea currents, flooding, erosion, and land conversion in the upper reaches. This time-series past DTM modeling can provide a 3D visualization of changes in the dynamic topography in SAL. Vertical deformation is the movement of land up (uplift) or down (subsidence) due to tectonic movements. Even though the area is experiencing subsidence tectonically, other parameters influence it more dominantly. Another parameter is sedimentation. Rapid sedimentation in the SAL is caused by the large amount of soil and mineral materials carried by river currents from upstream to downstream. The SAL is the downstream part of a combination of various upstream rivers, such as Citanduy, Cikonde, Cimeneng, Cibeureum, Sapuregel, and Donan. The addition of sedimentation forms new land (*aanslibbing*). The addition of the sedimentation rate to the DTM uses information from the Department of BBWS Citanduy. BBWS is the Indonesian government agency responsible for monitoring the Citanduy River area, including the SAL.

In this pattern of sediment distribution, it is clear that the river is the most significant contributor to sediment deposits in the SAL. The sediment concentration carried by the dominant river flow is carried into the lagoon at high tide, but at low tide, not all of the sediment carried by the tidal flow can be carried out by the current. Discharge events representing daily events indicate that the river currents are not strong enough to fight the tides. Meanwhile, almost all sediment is carried into the estuary at low tide. However, due to the current speed not being as strong as during high tide, the sediment still floating at low tide can be carried back into the lagoon before it reaches the open sea. The sediment supply from this river is a source of sediment that causes siltation in the SAL. The

process of merging the emergent land with the mainland continued until 2001.

Based on the sea level analysis, the pattern of changes in sedimentation formed in SAL can be seen. Sedimentation patterns tend to gather and form raised soil towards the east side of SAL. The direction of sedimentation movement can be seen from the shifting of the MSL line. Based on the time-series DTM modeling results, the MSL lines in SAL are very dynamic. The pattern of shoreline changes that occurred in SAL can be mapped. In 1978, SAL was very wide, and the mouth of the river was extensive, especially the Cibeureum River. Changes in the MSL line were seen in 1991, 2001, 2010, and 2021. The MSL line in 1991 changed due to sedimentation that formed, causing the MSL line to shift. The high sedimentation causes the emerging land initially separated from the mainland to merge into new land and widen over time, likewise, in 2001, 2010, and 2021. The high sedimentation rate causes the surface soil to become more comprehensive and changes the MSL line. The much-changing MSL line is on the east side of the SAL. It is caused by the direction of movement of sedimentation, which is more to the east side.

Most of the deposition occurred around the islands' lagoon area, with a maximum change in depth of about 0.6 m and an average change in depth within one year for the lagoon area of around 0.16 m. Most of the deposition occurred in the area around the lagoon and delta. This area becomes the entry and exit route for sediment into the body of the lagoon. Its close position to the Citanduy River causes the volume of sediment carried in at high tide to be very high. Then, at low tide, these sediments are still left in the area around the island. As a result, floating sediments are scattered in this area. Then, the shape of the gaps between islands, which are like straits, causes the flow that enters the gaps between these islands to be faster. However, the velocity

decreases when the flow meets an area with a broader cross-section. This decrease in speed causes much sediment carried by fast currents to gather in areas near the island where the flow is slower, so the deposition is focused on this area when the flow speed slows down.

The SAL has a very high sedimentation rate. It conducted research related to sedimentation based on the field surveys. Based on these results, sedimentation significantly increased from 0 – 40 mg/l in 1978 to 40 – 320 mg/l in 2012. A report from BBWS 2012 stated that the total sediment supply in SAL reached 9.14 million tons/year, carried by the flow from the Citanduy, Cimeneng, and Cikonde rivers (BBWS, 2012). The Citanduy, Cimeneng, and Cikonde rivers are the main contributors to the SAL sedimentation process, with an average discharge from the Citanduy River of 140 m³/s (range 80 – 300 m³/s) stated that the particles carried came from Mount Galunggung dust, andosol, and latosol agricultural soil containing clay, quartz sand, pesticide and fertilizer compounds, and waste from both industry and households. The total volume of sediment entering SAL is estimated to be around 1 million m³/year (Pawitan, 2002).

Apart from sedimentation particles carried by water flow, the sedimentation process is also influenced by tides. SAL is influenced by different water masses, namely seawater (Hindian Ocean) and freshwater from rivers that empty into the lagoon. During high tide conditions, the flow of particles from the Citanduy, Cimeneng, Cikonde, Cikujang, and Cibereum rivers headed to the south is forced by the tidal flow of seawater so that they return to the north. At low tide, the river's swift currents carry particles that will then settle in the SAL. This continuous process causes the SAL to become increasingly narrow. SAL experienced very dynamic changes due to particle sedimentation carried by the flow of the Citanduy, Cimeneng, and Cikonde rivers. The area of the SAL in 1903 was 6,450 ha and was getting narrower until 2003 (BBWS, 2012). The area was estimated at 600 ha. It occurs due to the accumulation of sediment particles in new land. The silting processes are concentrated around deltas and lagoons near river mouths. The delta is estimated to increase in size and eventually be connected.

The SAL is continuously degraded due to high levels of deposition. Precipitation in these waters has resulted in siltation and narrowing of the area. The water area of the SAL in 1903 was 6,450 ha. However, in 1939, it was reduced to 6,060 ha. Around 1971, the area of SAL shrank back to

4,290 ha. This continued until 1984, when the area of the lagoon became 2,906 ha. In 1994, it shrank to 1,575 ha. Depreciation is still happening, so in 2003, it reached 600 ha. In 19 years, there has been a decrease in the area of the lagoon by 2,306 ha or 121.4 ha per year (Ardli, 2008; Hakiki et al., 2021). The shrinkage of the SAL is mainly due to the high amount of sediment material entering the lagoon. The presence of raised soil caused by sedimentation causes the growth of mangroves. It follows the growing conditions for mangrove vegetation, namely muddy soil protected from waves and influenced by tides. The high silt deposition becomes a suitable area for mangrove vegetation to grow. The raised soil in the eastern part of Karanganyar has calm water conditions, so mangroves with the *Rhizophora sp.* species grow.

The shrinkage of the SAL is caused by tidal asymmetry in the SAL, which results in the current velocity during high tide conditions being more dominant than the current velocity during low tide conditions. Under these conditions, the sediment supply from the Citanduy River will be carried deep into the lagoon due to the large tidal currents. Then, smaller ebb currents mean that not all of the sediment brought in at high tide can be completely carried out of the lagoon area. The sediment left behind will settle when the flow slows down due to phase changes from high and low tides.

The reduction in the SAL is due to sedimentation, changes in tidal phases, and current patterns (Hakiki et al., 2021). The results of their research indicated a tidal asymmetry in the SAL, which resulted in currents at high tide being more dominant than currents at low tide. As a result, sediments originating from the river will be carried far into the lagoon due to the large tidal currents. However, the smaller ebb currents mean that not all the sediment brought in at this tide can be completely carried out of the lagoon area. So that sediment remains in the lagoon area every time the tidal cycle occurs. Then, when entering the time of flow change from high tide to low tide, the sediment left in the lagoon area will settle because the flow velocity during this phase can be close to zero or the flow is almost silent. The consequence of this tidal asymmetry is that sediment deposition in the lagoon due to the sediment material carried by the Citanduy River discharge is quite significant. At high tide, it is observed that the flow from the Citanduy River is carried into the body of the lagoon due to being pushed by the tidal currents. Meanwhile, this river will flow into the sea along with other water masses in the lagoon at low tide.

While our modeling provides a novel insight into the historical dynamics of SAL, several limitations should be acknowledged. Firstly, the model relies on a constant sedimentation rate derived from a 2012 report. In reality, sedimentation rates may have varied non-linearly due to changes in land use upstream, extreme weather events, or dredging activities. Secondly, the vertical deformation rate was extrapolated from a 2017–2021 dataset, assuming a

linear trend over the past decades. Future research could refine this model by incorporating historical land-use data to estimate variable sediment loads and by analyzing longer-term geological data for more complex deformation patterns. Furthermore, validating the reconstructed DTMs with historical bathymetric charts or sediment core data, where available, would provide an independent assessment of the model's accuracy.

5. CONCLUSIONS

Time-series DTM can explain how the pattern changes from a location on the Earth's surface. DTM can explain the sedimentation process that occurs in the SAL. The ability of the DTM can easily explain how the profile of the height of the soil arises due to sedimentation in the area. In 1978, the vast and narrower SAL was seen. The continuous sediment flow at a very high rate causes deposition, so that the soil appears. The erosion in the Citanduy watershed contributes more particles to the downstream part of SAL. These particles make a significant contribution to sedimentation in SAL.

DTM (2021), vertical deformation (2017–2021), and rapid sedimentation data can be used to model the dynamic topography (1978–2021) in SAL. This dynamic topography modeling uses (1) parameters of sedimentation rate and volume obtained from BBWS 2012, (2) DTM 2021 extracted from ALOS-2 (2017), WorldView (2017), and integrates it with vertical deformation from Sentinel-1 (2017–2021) using the D-InSAR method.

The DTM 2021 has a spatial resolution of 1 m and has been validated in its vertical accuracy test (+17.6 cm) and its height difference test (~0 m) with a confidence level of 95 % (1.96 σ). The average

vertical deformation value is –0.0240 to –0.0320 m. DTMs (1978, 1991, 2001, 2010, and 2021) are conditions of dynamic topographic changes. They are carried out by checking the dynamics of shoreline changes and cross-section profiles. This comparison will visualize shapes, patterns, and deltas in the SAL and delta areas. Based on the time-series DTMs, the SAL from 1978 to 2021 is increasing due to sedimentation. New land has been raised in the SAL on the west side, which is getting more expensive, and an uplift elevation exists. Sedimentation is the main parameter that causes dynamic topography changes in SAL. It significantly impacts the formation of new land, which is more dominant than vertical deformation (tectonic). Sedimentation caused the land elevation of SAL to rise in 1978: 0.36 m, 1991: 0.97 m, 2001: 0.9 m, 2010: 2.0 m, and 2021: 1.8 m. Changes in land area appear to affect the position of the MSL line because it appears to shift from its initial position. The MSL line shifts to the east side of SAL.

Acknowledgements: *We thank the Indonesian National Research and Innovation Agency (BRIN) for supporting this independent research and P.T. Citra Bhumi Indonesia (CBI) for supporting this research data. This publication does not receive external or internal funding. Atriyon Julzarika is the main contributor to this paper.*

REFERENCES

- Akbar, M. R., Arisanto, P. A. A., Sukirno, B. A., Merdeka, P. H., Priadhi, M. M., Zallesa, S. (2020): Mangrove vegetation health index analysis by implementing NDVI (normalized difference vegetation index) classification method on sentinel-2 image data case study: Segara Anakan, Kabupaten Cilacap. IOP Conference Series: *Earth and Environmental Science*, **584** (1):012069. <https://doi.org/10.1088/1755-1315/584/1/012069>
- Ardli, E. R. (2008): *A trophic flow model of the Segara Anakan lagoon, Cilacap, Indonesia* [Dissertation]. Universität Bremen.
- Arroyo-Ortega, I., Chavarin-Pineda, Y., Torres, E. (2024): Assessing contamination in transitional waters using geospatial technologies: A review. *ISPRS International Journal of Geo-Information*, **13**(6). <https://doi.org/10.3390/ijgi13060196>
- ASPRS. *Accuracy Standards for Digital Geospatial Data*. The American Society for Photogrammetry and Remote Sensing. 2014. [https://doi.org/10.1016/S0033-3506\(98\)80082-6](https://doi.org/10.1016/S0033-3506(98)80082-6)
- BBWS, Kajian Penanganan Sedimen Segara Anakan melalui Check Dam dan Pengerukan (Study of Sediment Handling in Segara Anakan through Check Dam and Dredging). Workshop Penanganan Segara Anakan. 2012.
- De Luca, C., Bonano, M., Casu, F., Manunta, M., Manzo, M., Onorato, G., Zinno, I., Lanari, R. (2018): The parallel SBAS-DInSAR processing chain for the generation of national scale Sentinel-1 deformation time-series. *Procedia Computer Science*, **138**, pp. 326–331. <https://doi.org/10.1016/j.procs.2018.10.046>

- Dias, P., Catalao, J., Marques, F. O. (2018): Sentinel-1 InSAR data applied to surface deformation in Macaronesia (Cnaries and Cape Verde). *Procedia Computer Science*, **138**, pp. 382–387. <https://doi.org/10.1016/j.procs.2018.10.054>
- Dsikowitzky, L., Van der Wulp, S. A., Dwiytino, Ariyani, F., Hesse, K. J., Damar, A., Schwarzbauer, J. (2018): Transport of pollution from the megacity Jakarta into the ocean: Insights from organic pollutant mass fluxes along the Ciliwung River. *Estuarine, Coastal and Shelf Science*, **215**, pp. 219–228. <https://doi.org/10.1016/j.ecss.2018.10.017>
- Dudley, R. G. (2020): Segara Anakan Fisheries Management Plan. Segara Anakan Conservation and Development Project.
- Ghilani, C. D., Wolf, P. R. (2006): Adjustment Computations Spatial Data Analyses, 4th Edition. <https://doi.org/10.1038/ni1566>
- Guth, P. L., Van Niekerk, A., Grohmann, C. H., Muller, J.-P., Hawker, L., Florinsky, I. V., Gesch, D., Reuter, H. I., Herrera-Cruz, V., Riazanoff, S., López-Vázquez, C., Carabjal, C. C., Albinet, C., Strobl, P. (2021): Digital elevation models: terminology and definitions. *Remote Sensing*, **13** (18), 3581. <https://doi.org/10.3390/rs13183581>
- Guzzeti, F., Manunta, M., Ardizzone, F., Pepe, A., Cardinali, M., Zeni, G., Reichenbach, P., Lanari, R. (2009): Analysis of ground deformation detected using the SBAS-DInSAR technique in Umbria, Central Italy. *Pure and Applied Geophysics*, **166**, pp. 1425–1459. <https://doi.org/10.1007/s00024-009-0491-4>
- Hakiki, I. A., Sembiring, L. E., Nugroho, C. N. R. (2021): Sedimentation Analysis of Segara Anakan Lagoon using cohesive sediment transport numerical modelling. *Jurnal Teknik Hidraulik*, **12** (1), pp. 1–14. <https://doi.org/10.32679/jth.v12i1.642>
- Hoja, D., D'Angelo, P. (2010): Analysis of DEM combination methods using high resolution optical stereo imagery and interferometric SAR data. *International Archives of the Photogrammetry, Remote Sensing and Spatial Information Science*, Volume XXXVIII, Part 1, 2–5. <https://doi.org/10.1007/978-3-319-59489-7>
- Ismail, Suliztano, Hariyadi, S., Madduppa, H. (2018): Condition and mangrove density in Segara Anakan, Cilacap Regency, Central Java Province, Indonesia, *AACL Bioflux*, **11** (4) 1055–1068, <http://www.bioflux.com.ro/aac1>
- Julzarika, A., Djurdjani, D. (2019): DEM classifications: opportunities and potential of its applications. *Journal of Degraded and Mining Lands Management* **6** (4). <https://doi.org/10.15243/jdmlm.2019.064.1897>
- Julzarika, A., Harintaka, H. (2019): Utilization of Sentinel -1 satellite for vertical deformation monitoring in Semangko Fault – Indonesia. (ACRS) – *The 40th Asian Conference on Remote Sensing, October 14–18, 2019/Daejeon Convention Center (DCC), Daejeon, KoreaWeA2-31*, pp. 1–7.
- Julzarika, A., Aditya, T., Subaryono, S., Harintaka, H., Dewi, R. S., Subehi, L. (2021): Integration of the latest digital terrain model (DTM) with Synthetic aperture radar (SAR) bathymetry. *Journal of Degraded and Mining Lands Management*, **8** (3), 2502–2458. <https://doi.org/10.15243/jdmlm.2021.083.2759>
- Julzarika, A., Aditya, T., Subaryono, S., Harintaka, H. (2022): Dynamics topography monitoring in Peatland using the latest digital terrain model. *Journal of Applied Engineering Science*, **20** (1), 246–253. <https://doi.org/10.5937/jaes0-31522>
- Karim, M., Maanan, M., Maanan, M., Rhinane, H., Rueff, H., Baiddier, L. (2019): Assessment of water body change and sedimentation rate in Moulay Bousselham wetland, Morocco, using geospatial technologies. *International Journal of Sediment Research*, **34**(1), 65–72. <https://doi.org/10.1016/j.ijsrc.2018.08.007>
- Li, X., Shen, H., Feng, R., Li, J., Zhang, L. (2017): DEM generation from contours and a low-resolution DEM. *ISPRS Journal of Photogrammetry and Remote Sensing*, **134**, pp. 135–147, <https://doi.org/10.1016/j.isprsjprs.2017.09.014>
- Li, Z., Zhu, C., Gold, C. (2004): *Digital Terrain Modeling: Principles and Methodology*. CRC Press, Boca Raton. <https://doi.org/10.1201/9780203357132>
- Liosis, N., Marpu, P. R., Pavlopoulos, K., Ouarda, T. B. M. J. (2018): Ground subsidence monitoring with SAR interferometry techniques in the rural area of Al Wagan, UAE. *Remote Sensing of Environment*, **216**, pp. 276–288. <https://doi.org/10.1016/j.rse.2018.07.001>
- Maune, D. F., Nayegandhi, A. (2018): *Digital Elevation Model Technologies and Applications: The DEM Users Manual*. American Society for Photogrammetry and Remote Sensing.
- Mazhari, S. A. (2010): An introduction to forensic geosciences and its potential for Iran. *Journal of Geography and Geology*, **2**(1). <https://doi.org/10.5539/jgg.v2n1p77>
- Nico, G., Leva, D., Fortuny-Guasch, J., Tarchi, D., Antonello, G. (2005): Generation of digital terrain models with a ground-based SAR system. *IEEE Transactions on Geoscience and Remote Sensing*, **43**(1). 45–49. <https://doi.org/10.1109/TGRS.2004.838354>
- NOAA (2024). *What is a lagoon?* National Ocean Service website, National Oceanic and Atmospheric Administration. <https://oceanservice.noaa.gov/facts/lagoon.html#:~:text=Although%20lagoons%20are%20well%20defined,exposed%20locations%20on%20the%20shore.,06/16/24>.
- Ongkosongo, O. (1986): Some harmful stresses to the Seribu coral reefs, Indonesia, *Proc. MAB – COMAR Region Workshop on Coral Reef Ecosystems*.
- Paul, A. Kr., Islam, Sk. M., Jana, S. (2014): An assessment of physiographic habitats, geomorphology and evolution of Chilika Lagoon (Odisha, India) using geospatial technology. In: C. W. Finkl & C. Makowski (Eds.), *Remote Sensing and Modeling: Advances in Coastal and Marine Resources*. pp. 135–160. Springer International Publishing. https://doi.org/10.1007/978-3-319-06326-3_6
- Pawitan, H. (2002): Eco-hydrological measures for the management of the Segara Anakan Lagoon basin in West Java, Indonesia. *International Symposium on Low-Lying Coastal Areas – Hydrology and Integrated Coastal Zone Management*, September 2002.
- Prayudha, B., Siregar, V., Ulumuddin, Y. I., Suyadi, Prasetyo, L. B., Agus, S. B., Suyarso, Anggraini, N. (2021): The application of Landsat imageries and mangrove vegetation

index for monitoring mangrove community in Segara Anakan Lagoon, Cilacap, Central Java. *IOP Conference Series: Earth and Environmental Science*, 944 (1). <https://doi.org/10.1088/1755-1315/944/1/012039>

Ruffell, A., & McKinley, J. (2008): *Geoforensics*. John Wiley & Sons, Ltd. ISBN: 978-0-470-05735-3

Şenol, H. İ., Kaya, Y., Yiğit, A. Y., Yakar, M. (2024): Extraction and geospatial analysis of the Hersek Lagoon shoreline with Sentinel-2 satellite data. *Survey Review*, **56** (397), 367–382. <https://doi.org/10.1080/00396265.2023.2257969>

Spaulding, M. L. (1994): Chapter 5: Modeling of circulation and dispersion in coastal lagoons. In: B. Kjerfve (Ed.),

Elsevier Oceanography Series, Vol. **60**, pp. 103–131. Elsevier. [https://doi.org/https://doi.org/10.1016/S0422-9894\(08\)70010-2](https://doi.org/https://doi.org/10.1016/S0422-9894(08)70010-2)

Strozzi, T., Klimeš, J., Frey, H., Caduff, R., Huggel, C., Wegmüller, U., Alejo Cochachin, R. (2018): Satellite SAR interferometry for the improved assessment of the state of activity of landslides: A case study from the Cordilleras of Peru. *Remote Sensing of Environment* **217**, pp. 111–125. <https://doi.org/10.1016/j.rse.2018.08.014>

Wilson, J. (2012): Digital terrain modeling. Regional Assessment of Global Change Impacts: The Project GLOWA-Danube, *Geomorphology* **137** (1), 69–74. https://doi.org/10.1007/978-3-319-16751-0_7

Резиме

МОДЕЛИРАЊЕ НА ДИНАМИКАТА НА ЛАГУНА СО КОРИСТЕЊЕ НА ДИГИТАЛЕН МОДЕЛ НА ТЕРЕНОТ СО ДЕТАЛНИ ВРЕМЕНСКИ СЕРИИ

Atriyon Julzarika^{1*}, Nanin Anggraini¹, Argo Galih Suhadha^{1,2}, Danang Budi Susetyo^{1,3}, Rahmadi Rahmadi¹, Bayu Prayudha¹, Nugroho Purwono¹, Yaya Ihya Ulumuddin

¹Национална агенција за истражување и иновации (BRIN), Џибинонг, Индонезија

²Универзитет Тохоку, Сендаи, Јапонија

³Технички универзитет Јулдиз, Истанбул, Турција

*verbhakov@yahoo.com

Клучни зборови: DTM и вертикална деформација; динамична лагуна; SAL; динамика на топографија; брза седиментација

Лагуната е природна појава формирана на устието на река поради динамиката на седиментацијата на реката, струите, вертикалната деформација, брановите и плимата и осеката. Во лагуните доминираат меки почви, па затоа нивната топографија е динамична. Лагуната Сегара Анакан (SAL) е област која доживува динамична топографија предизвикана од брзата седиментација. Промените во динамиката на топографијата на делтата во минатото можат да се следат преку временските серии на дигиталниот модел на теренот (DTM), извлечени од поранешните податоци на DTM. Периодот на набљудување беше 1978–2021 година. Целта на ова проучување е да се моделира динамиката на топографијата (1978–2021) во SAL според податоците на DTM за вертикалната деформација и седиментацијата. Ова динамичко моделирање на топографијата користи (1) параметри на брзината и волуменот на седиментација добиени од центарот на речниот слив – Балаи Бесар Вилаја Сунгаи (BBWS) 2012, (2) DTM за 2021 извлечен од ALOS-2 (2017) и интегриран со вертикалната деформација од Sentinel-1 (2017–2021) со користење на методот на диференцијален интерферометриски синтетички радар за апертури (D-InSAR). DTM-ите (1978, 1991, 2001 и 2010) се

извлечени со користење на геопросторен пристап на вештачење базиран на топографско моделирање на DTM 2021, вертикална деформација (2017–2021) и податоци за брза седиментација. Користена е стапката на седимент што влегува во SAL од реката Цитандуј (8,05 милиони тони годишно), реката Чимененг (0,87 милиони тони годишно) и реката Циконде (0,22 милиони тони годишно), со вкупен принос на седимент од 9,14 милиони тони годишно. DTM 2021 има просторна резолуција од 1 m и е валидиран со тестот за вертикална точност (+17,6 cm) и тестот за висинска разлика (~0 m) со ниво на доверба од 95% (1,96 σ). Просечната вредност на вертикалната деформација е од –0,0240 до –0,0320 m. Добиените резултати даваат информации за динамиката на топографијата (1978–2021). DTM (1978–2021) ги визуелизираат промените на динамиката на топографијата во SAL. Тие се добиваат со проверка на динамиката на промените на брегот и профилите на попречните пресеци за да се утврди соодветноста на облиците и моделите (лагуна и делта). Седиментацијата е најзначајниот параметар што влијае на динамиката на топографијата во SAL.